

Supplementary information

Non-Line-of-Sight Synthesis and Characterization of a Conformal Submicron-Thick Cationic Polymer Deposited on 2D and 3D Substrates

Hunter O. Ford,¹ Brian L. Chaloux,² Battogtokh Jugdersuren,³ Xiao Liu,⁴ Christopher A. Klug,² Joel B. Miller,⁵ Xiaobing Zuo,⁶ Michael W. Swift,⁷ Michelle D. Johannes,⁷ Jeffrey W. Long,² Debra R. Rolison^{2*} and Megan B. Sassin^{2*}

*Corresponding Authors: E-mail: megan.sassin@nrl.navy.mil; debra.rolison@nrl.navy.mil

¹ NRL–NRC Postdoctoral Associate in the Chemistry Division, U.S. Naval Research Laboratory, Washington, DC 20375, USA

² Chemistry Division, U.S. Naval Research Laboratory, Washington, DC 20375, USA

³ Jacobs Engineering Group, Hanover, MD 21076, USA

⁴ Acoustics Division, U.S. Naval Research Laboratory, Washington, DC 20375, USA

⁵ Emeritus, Chemistry Division, U.S. Naval Research Laboratory, Washington, DC 20375, USA

⁶ X-ray Science Division, Argonne National Laboratory, Lemont, IL 60439, USA

⁷ Materials Science & Technology Division, U.S. Naval Research Laboratory, Washington, DC 20375, USA

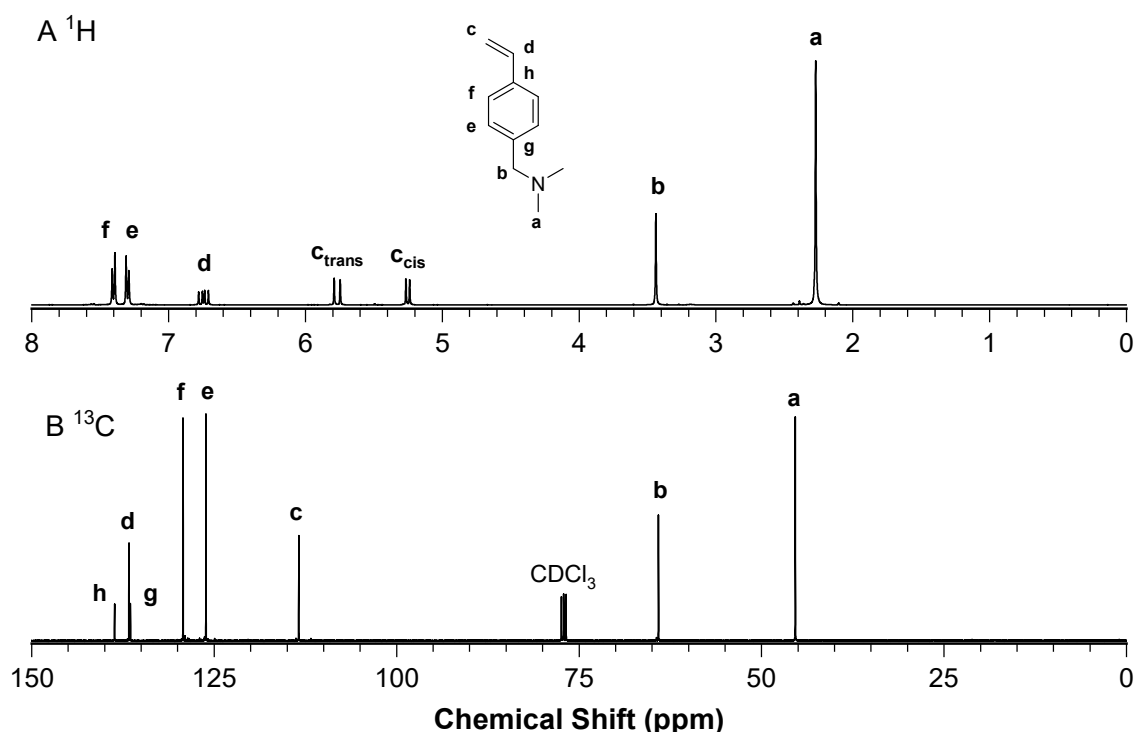


Fig. S1 NMR spectra of 4-dimethylaminomethylstyrene in CDCl₃: (A) ¹H and (B) ¹³C.

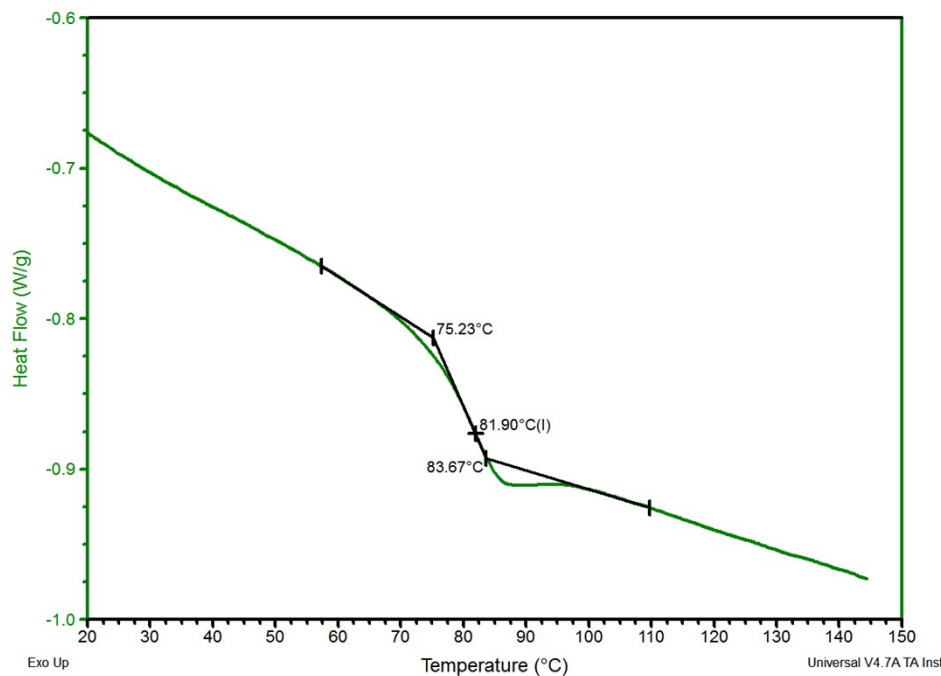


Fig. S2 Differential scanning calorimetry heating curve (20K min^{-1}) of pDMAMS prepared from neat free radical polymerization of DMAMS with AIBN at 100°C , with calculation of T_g (82°C) as the inflection point in the second-order thermal transition.

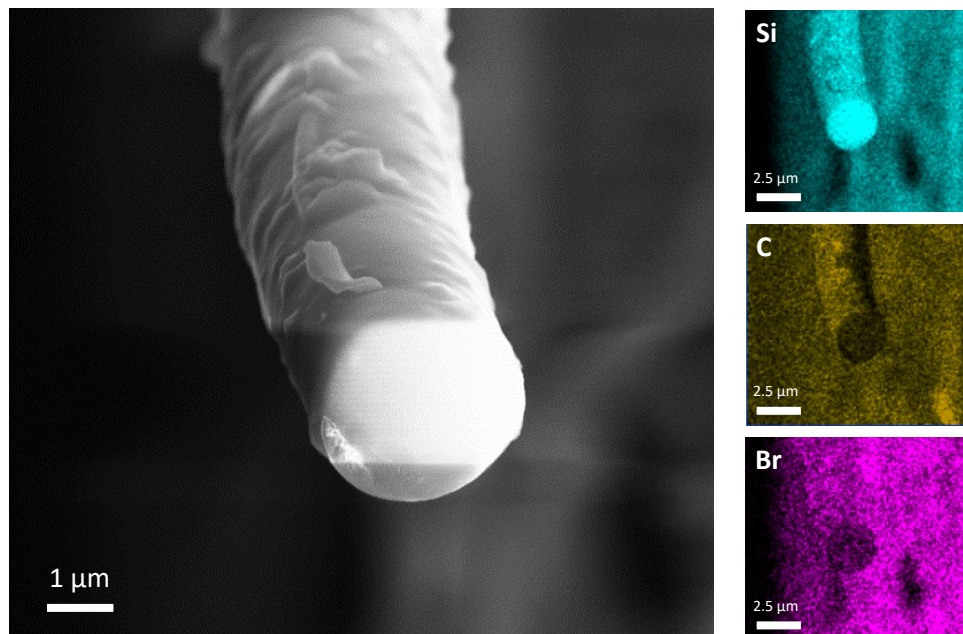


Fig. S3 SEM–EDX images of silica fiber paper coated with pDMAMS⁺. The bright Si and diminished C/Br signal at the shorn fiber cross-section and the inverse along the length of the fiber indicate conformal coating.

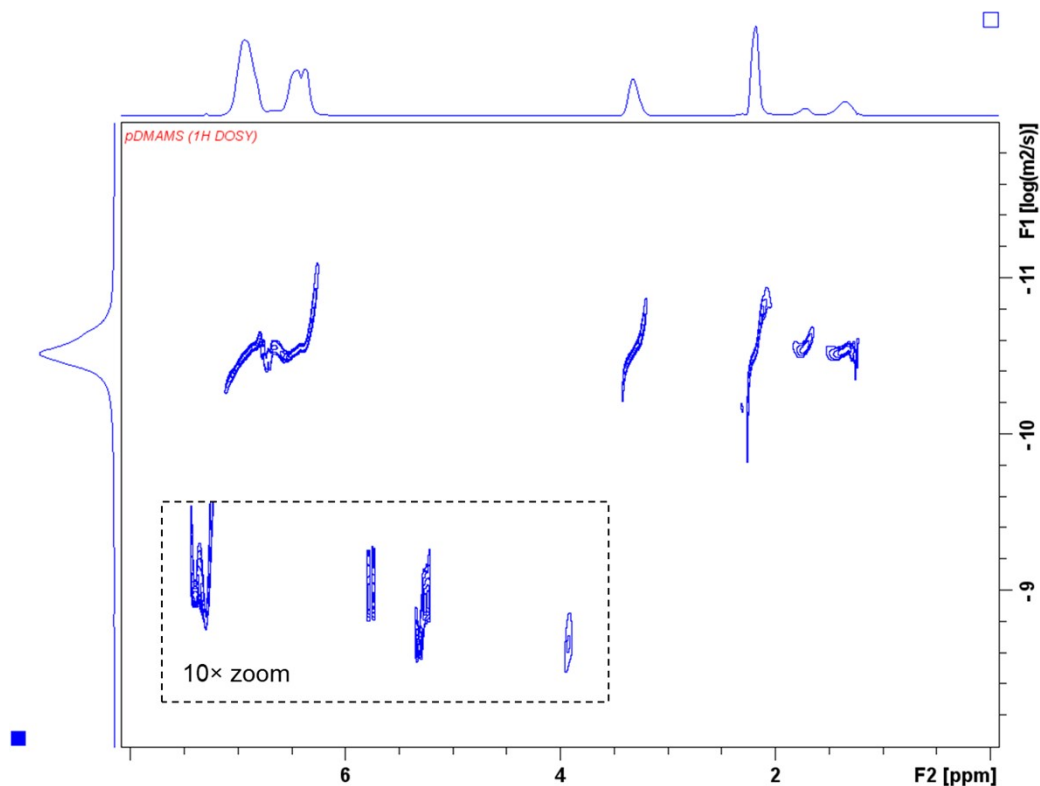


Fig. S4 ^1H DOSY pseudo-2D NMR spectrum of bulk-synthesized pDMAMS dissolved in CDCl_3 . Inset is zoomed in to show peaks for CHCl_3 and residual monomer, which are significantly weaker than the polymer peaks.

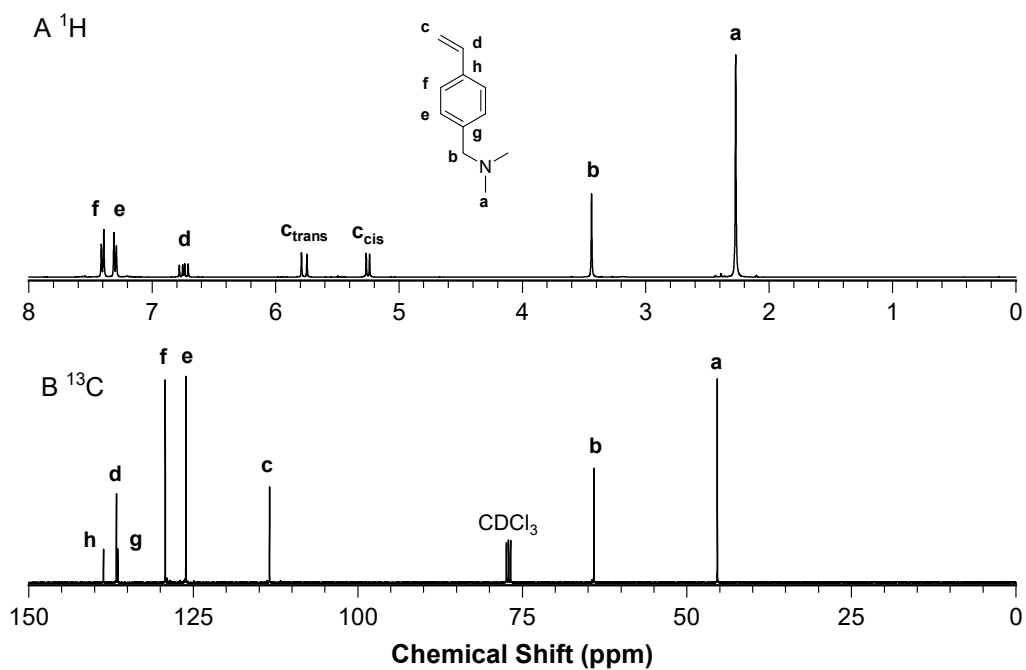


Fig. S5 (A) ^1H and (B) ^{13}C NMR spectra of pDMAMS prepared from neat free-radical polymerization of DMAMS with AIBN at 100°C . Trace monomer (<1 mol%) is visible in the ^1H NMR spectrum.

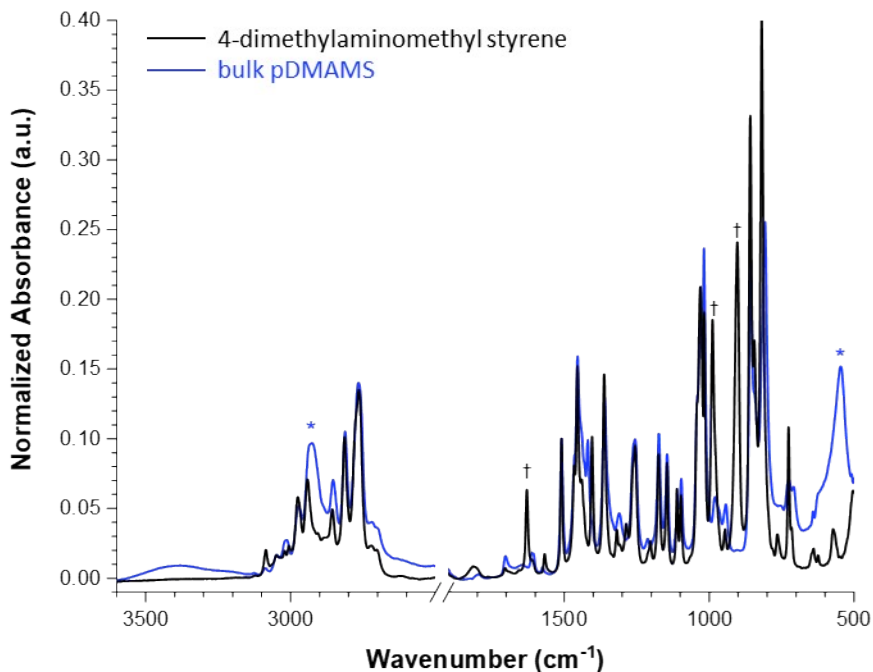


Fig. S6 Overlaid ATR-FTIR spectra of 4-dimethylaminomethylstyrene (DMAMS monomer, black) and bulk-synthesized pDMAMS (blue) with intensities normalized to the peak at 1510 cm^{-1} , which remains invariant over the course of polymerization. Features present in pDMAMS but not in the monomer are annotated with a blue asterisk (*) while those present in DMAMS but not the polymer are annotated with a black dagger (†).

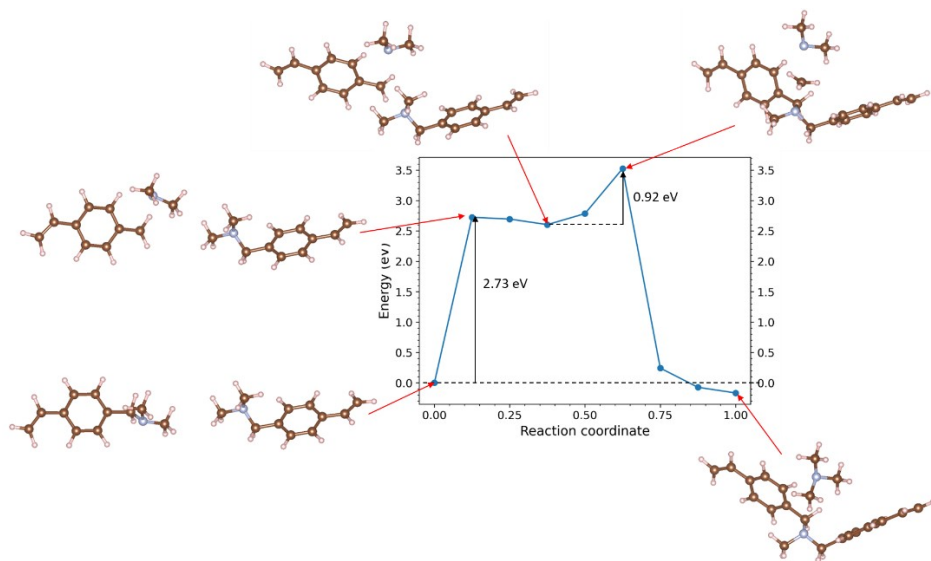


Fig. S7 Density functional theory calculations and associated structures detailing potential annealing-induced cross-linking reactions.

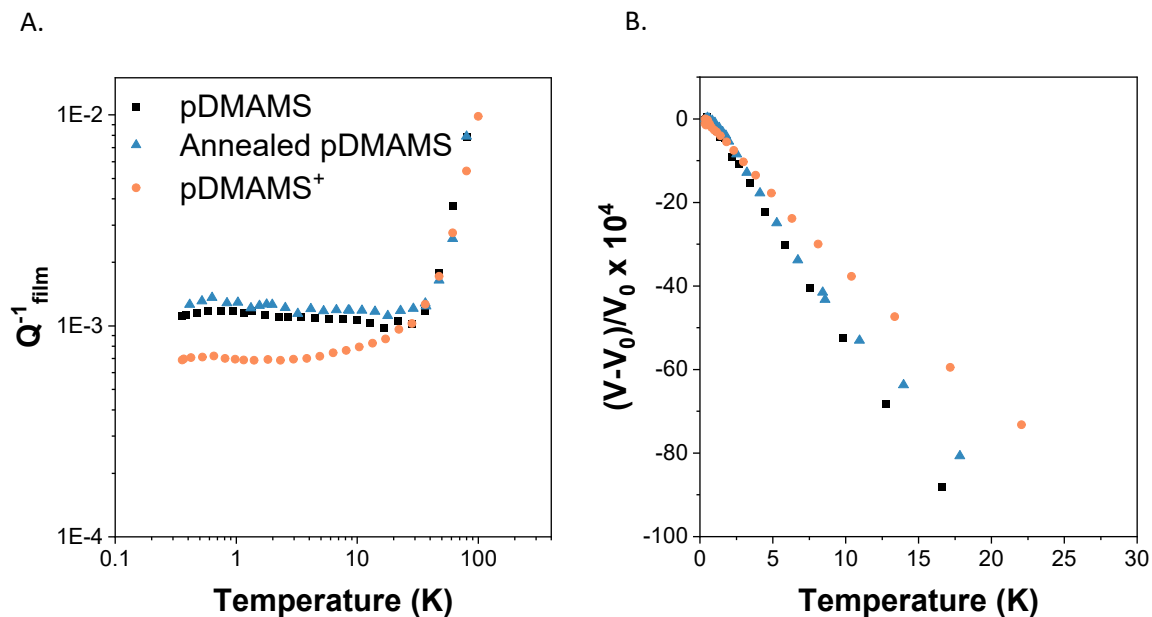


Fig. S8 Mechanical properties of pDMAMS in the as-deposited, annealed, and alkylated states. (A) Film loss/internal friction (Q^{-1}); (B) relative change in the speed of sound.

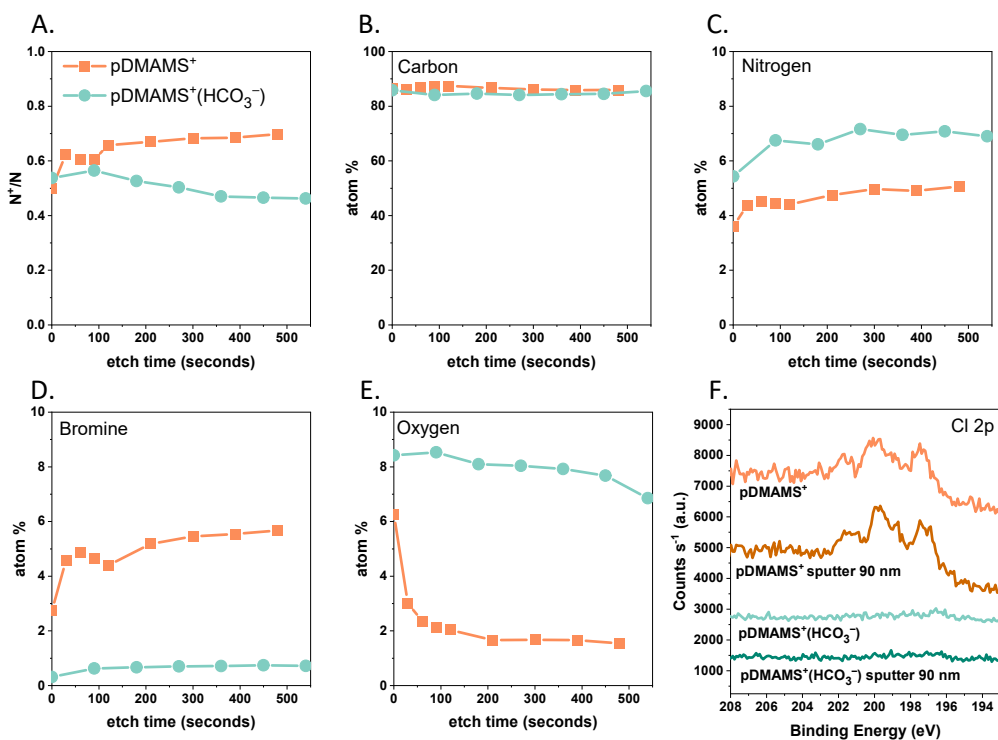


Fig. S9 XPS depth-profiling results for different elements for pDMAMS⁺ and pDMAMS⁺(HCO₃⁻). (A) ratio of quaternary ammonium N^+ to amine N (measurement of functionalization); (B) Carbon; (C) Nitrogen; (D) Bromine; (E) Oxygen; (F) Surface and 90 nm (500 s sputtered) Cl spectra.

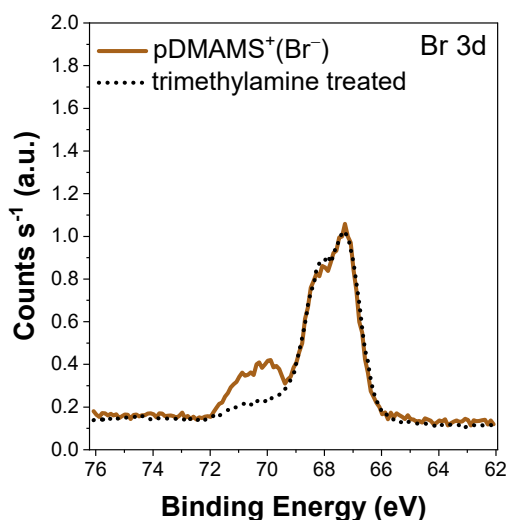


Fig. S10 XPS spectra of pDMAMS⁺ and pDMAMS⁺ treated with trimethylamine.

Table S1 Atomic percentages as determined via XPS for various pDMAMS compositions.

| Sample | Atomic % | | | | | | | % N as N ⁺ | % Br as Br ⁻ |
|---|---------------|---------------|----------------------------|---------------|---------------|----------------------------|----------------|-----------------------------|-------------------------------|
| | C (286 eV) | N (399 eV) | N ⁺ (402 eV) | O (530 eV) | Br (69 eV) | Br ⁻ (67 eV) | Cl (200 eV) | | |
| pDMAMS | 81.80 | 3.24 | — | 14.80 | — | — | — | — | — |
| pDMAMS ⁺ | 88.30 | 1.64 | 3.06 | 3.61 | 0.46 | 2.40 | 0.50 | 65.1 | 83.9 |
| pDMAMS ⁺ (Br ⁻) | 87.83 | 1.65 | 3.09 | 3.64 | 0.56 | 2.29 | 0.90 | 65.1 | 80.3 |
| pDMAMS ⁺ (Br ⁻) amine treated | 88.64 | 1.88 | 3.51 | 3.24 | 0.27 | 2.47 | — | 65.3 | 90.1 |
| pDMAMS ⁺ (HCO ₃ ⁻) | 83.00 | 3.73 | 2.86 | 10.30 | — | — | — | 43.4 | — |

Calculation of IEC (ion exchange capacity in mEq g⁻¹)

$$IEC = DF * \frac{1000 \text{ mmol}}{MW_{\text{monomer}} + \frac{MW_{\text{alkyl halide}}}{\#FG}} \quad \text{EQ. S1}$$

where:

MW_{monomer} = molecular weight of the monomer (e.g., DMAMS = 161.25 g mol⁻¹)

DF (degree of functionalization) = fraction of monomers that have been quaternized (e.g., 95%)

MW_{alkyl halide} = molecular weight of the quaternization agent (e.g., 1-bromo-3-chloropropane = 157.44 g mol⁻¹)

#FG (number of functional groups) = number of reactive groups (e.g., halides) per quaternization agent (e.g., 1-bromo-3-chloropropane = 2)

Calculation of cross-linking density

For pDMAMS⁺(Br⁻). Known: 65.1% N is N⁺, 80.3% Br is Br⁻. Assume basis of 100 nitrogens. For simplicity, treat Cl as Br as it behaves the same way chemically. Set up system of equations where x is the number of cross-links, y is the number of monolinks. Each cross-link has two N⁺ and two Br⁻. Each monolink (assuming one halide reacts with N and the other halide remains attached to the other end of the propyl group) contains one N⁺, one Br⁻ and one Br.

System of equations to solve:

$$65 = 2x + y \quad \text{EQ. S2A}$$

(Number of N⁺ must add to 65 assuming a 100 N basis)

$$0.197 = y/(2y + 2x) \quad \text{EQ. S2B}$$

(the percentage of Br relative to Br + Br⁻ must be 19.7%)

Solving yields x = 24.5 and y = 15.9.

Therefore, roughly 49% of all N (and therefore 49% of all DMAMS monomers) are participating in a cross-link as N⁺. ~16% of N is in a monolink as N⁺, and 35% of N remains as an amine.

From these calculations, for every mol of N in the polymer film, 0.4 mol of 1-chloro-3-bromopropane is reacted into the film, with 0.24 mol of 1-chloro-3-bromopropane reacting at both ends, 0.16 mol reacting at only one end.

Additional GISAXS/GIWAXS figures, equations, and modeling results

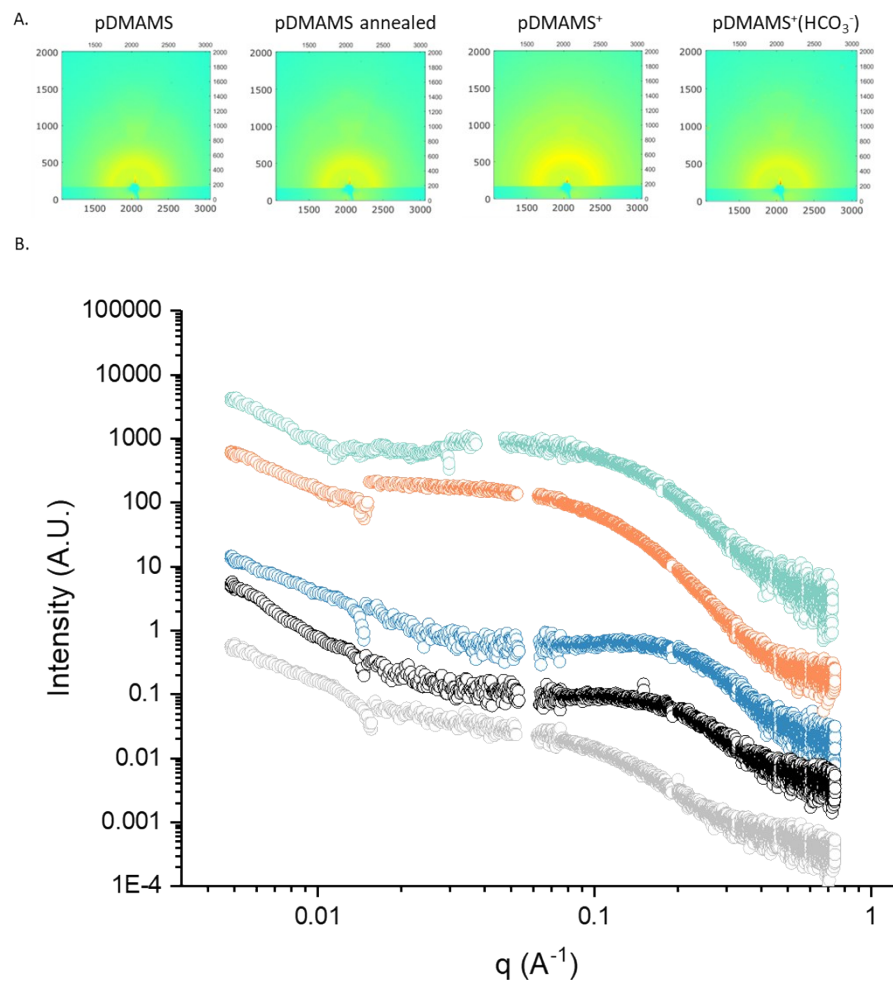


Fig. S11 (A) 2D GIWAXS patterns of various pDMAMS films. (B) 1D vertical slice GISAXS spectra taken from 2D GISAXS patterns in Fig. 6.

Table S2 Structure-independent multi-level unified fit model parameters for fit GISAXS spectra.

| Sample | G_1 (cm^{-1}) | R_{g1} (nm) | P_1 | B_1 (cm^{-1}) | G_2 | R_{g2} (nm) | P_2 | B_2 (cm^{-1}) | background |
|--|-------------------------------|------------------|-------|-------------------------------|-------|------------------|-------|-------------------------------|------------|
| pDMAMS | 10568 | 81.3 | 2.6 | 4.8E-3 | 6.2 | 3.5 | 2 | 1.2E-2 | 1.85 |
| Annealed pDMAMS | 2185 | 65.7 | 2.1 | 3.8E-3 | 0.07 | 1.5 | 1.7 | 2.3E-2 | 1.00 |
| pDMAMS ⁺ | 8195 | 48.1 | 2.59 | 7.6E-3 | 99.0 | 10.5 | 3.76 | 4.5E-5 | 1.80 |
| pDMAMS ⁺ (HCO ₃ ⁻) | 3143 | 99.0 | 1.69 | 4.0E-2 | 42.0 | 7.3 | 3.2 | 2.5E-4 | 0.70 |

$$I(Q) = \sum_{i=1}^n \left(G_i \exp\left(-\frac{q^2 R_{g,i}^2}{3}\right) + B_i \exp\left(-\frac{q^2 R_{g,i+1}^2}{3}\right) \right) q_i^{* P_i} \quad \text{EQ. S3A}$$

$$q^* = \frac{q}{\left\{ \text{erf}\left(\frac{kqR_{g,i}}{\sqrt{6}}\right) \right\}} \quad \text{EQ. S3B}$$

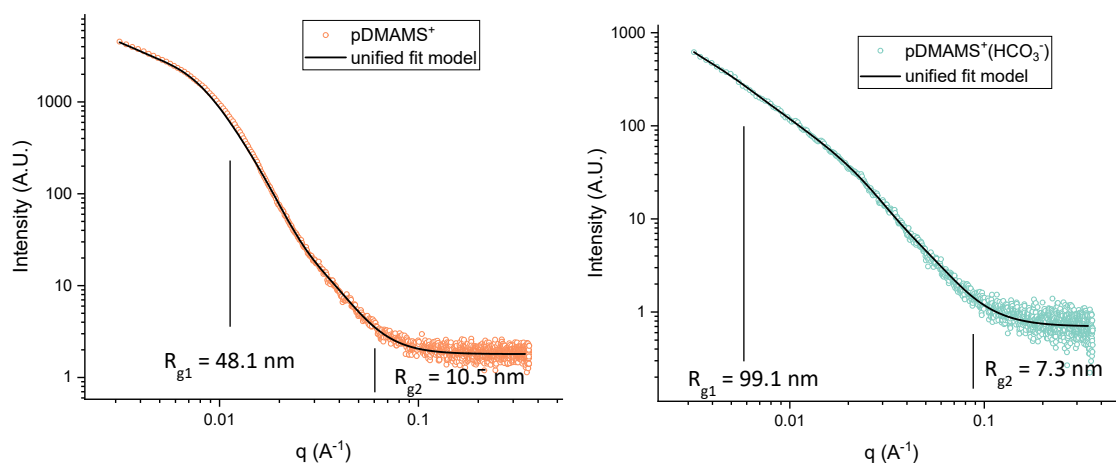


Fig. S12 pDMAMS⁺ and pDMAMS⁺(HCO₃⁻) GISAXS spectra and unified fit models with R_g length scales denoted.